



CHAPTER IV

EFFECT OF INTERNAL VOIDS ON INDUCED DIPOLE IN HDPE AND PP FILMS BY BLOWING AGENT COMPRESSION MOLDING

4.1 Abstract

The investigation of the effect of the internal voids induced in non-polar polymers on dielectric behavior was focused. The voided HDPE and PP films were fabricated by blowing agent compression molding (azodicarbonamide or ACA). The void size and foam density were controlled by varying blowing agent concentrations. Optical microscope micrographs showed the uniform dispersion of spherical voids. Thermal properties of voided films were not different compared to those of dense films. The dielectric constants of voided films decreased according to dielectric mixing rule. Serial model confirmed the connectivity of 0–3 void–polymer composites describes the uniform distribution of voids with closed air-gaps. Measurement of piezoelectric coefficient presented that the internal voids can enhance piezoelectric in non-polar polymers.

4.2 Introduction

Dipole moment of polar polymers arises from the orientation of the dipole in the field direction and results in orientational polarization. However, there is no dipolar alignment in non-polar polymers (Nalwa, H.S., 1995). To create the dipolar orientation in non-polar polymers, the presence of impurities such as void is necessary.

Nowadays, the using of foam-enhancing additives or blowing agents to produce foamed or cellular plastics is growing in applications. Small amount of blowing agent can produce the bubbles in a wide range of polymers. Azodicarbonamide or ACA is the most popular chemical blowing agent. It enjoys the most widespread use in commercial polyolefin foam production. It decomposes in a narrow temperature range approximately 200-210°C. The gas it releases, which

consists mostly of nitrogen and carbonmonoxide, does not cause undesirable foam shrinkage (Quinn, S., 2001).

High density polyethylene (HDPE) and Polypropylene (PP) are non-polar thermoplastic polymers. They consumed the high amount of the world synthetic resin production and their usage continues to grow. Nowadays, considerable attention for electret and piezoelectric applications is focused on thermoplastic polymers such as isotactic polypropylene (i-PP).

This work was focused on the effect of internal voids induced in HDPE and PP films on dielectric behaviors. ACA was used to create the internal voids by compression molding method. Subsequently, morphology of voided films was observed using Optical Microscope (OM). The dielectric constant and dielectric loss were measured as a function of frequency range from 1 kHz to 1 MHz and as a function of temperatures. Piezoelectric and ferroelectric properties obtained from voided films were compared to those of dense polymers films. Other physical, thermal and mechanical properties, are herein discussed.

4.3 Experimental

4.3.1 Preparation of Dense Films

The dense HDPE and PP films were produced by a compression molding method.

4.3.1.1 Dense HDPE film

HDPE pellets was pre-heated at 135 °C for 8 minutes and compressed at 200 °C and load 15 tons for 10 minutes. The film was kept in the mold until it was cooled down to 50 °C.

4.3.1.2 Dense PP film

PP pellets was pre-heated at 170 °C for 8 minutes and compressed at 200 °C and load 15 tons for 10 minutes. The film was kept in the mold until it was cooled down to 50 °C.

4.3.2 Preparation of Voided Films

The voided HDPE and PP films were produced by a compression molding method. The polymer–blowing agent compounds were blended with the Brabender mixer. The dried ACA was ground into powder and screened through a sieve (mesh #325) before using. ACA has decomposition temperature range 200-210 °C and gas volume is 215-225 ml/g.

4.3.2.1 *Voided HDPE films*

ACA and HDPE pellets were homogeneously blended with the Brabender mixer which set the rotor speed at 45 rpm and temperature at 145 °C. The temperature of molten compounds was 138.5-141 °C. Concentrations of 0.5%, 1%, 1.5%, 2% and 2.5% were used on the basis of the total weight of HDPE. Compounds were pre-heated and compressed at the same condition as dense HDPE film.

4.3.2.2 *Voided PP films*

ACA and PP pellets were homogeneously blended with the Brabender mixer which set the rotor speed at 45 rpm and temperature at 175 °C. The temperature of molten compounds was 167.2-170.5 °C. Concentrations of 0.5%, 1%, 1.5% and 2% were used on the basis of the total weight of PP. Compounds were pre-heated and compressed at the same condition as dense PP film.

The morphology was observed by Optical Microscope (OM) and density was characterized by Gas Pycnometer. The melting and crystallization behaviors and thermal stability were characterized by DSC and TGA, respectively. The mechanical properties was performed by Universal Testing Machine. The electrical properties including dielectric strength, dielectric constant, dielectric loss, piezoelectric coefficient and hysteresis loop were measured.

4.4 Results and Discussion

4.4.1 Films Fabrications

Dense and voided HDPE and PP films were prepared by compression molding technique. Dense and voided HDPE films of 556-656 μm and PP films of 553-673 μm thickness were obtained.

Figure 4.1 shows the images of dense and voided HDPE films with different concentrations of ACA. At 2.5 % ACA, the irregular and large voids were observed.

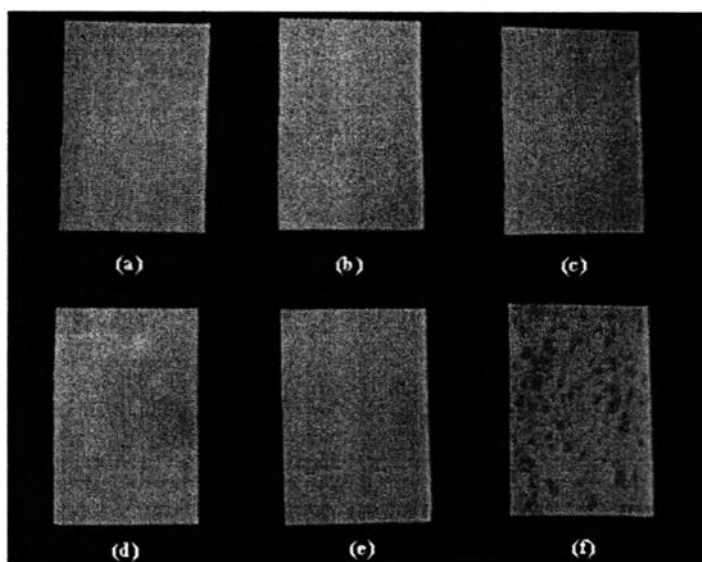


Figure 4.1 Images of HDPE films: (a) dense, (b) voided of 0.5 % ACA , (c) voided of 1 % ACA, (d) voided of 1.5 % ACA, (e) voided of 2 % ACA, and (f) voided of 2.5 % ACA.

Figure 4.2 shows the images of PP films. Dense PP film was translucent while voided films were opaque. The irregular and large voids were observed at 2 % ACA.

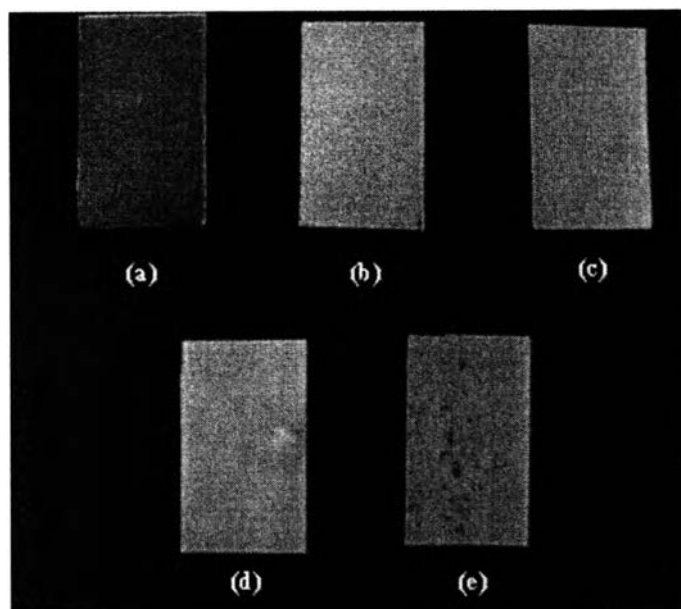


Figure 4.2 Images of PP films: (a) dense, (b) voided of 0.5 % ACA, (c) voided of 1 % ACA, (d) voided of 1.5 % ACA, and (e) voided of 2 % ACA.

From all images, the colors of the voided films were observed the changes. However, the voided structure and cell sizes cannot be seen clearly from the images. So the Optical microscope (OM) was used to study the morphology and void distribution.

4.4.2 Films Characterizations

4.4.2.1 *Physical Properties*

A. Morphology

OM micrographs of voided HDPE films with various concentrations of blowing agent are shown in Figure 4.3. The voided HDPE films usually feature spherical with closed-cell structure. Increasing blowing agent concentration seemed to give smaller cell sizes. However, the increasing of ACA concentration up to 2.5 % showed irregular voids. For a certain foam volume, the fewer large cells, the greater in stability was observed. This energy minimization factor favors cell coalescence. Therefore, to reach a dynamical stability, smaller bubbles tended to agglomerate into larger bubbles (Zhang, Y. *et al.*, 2003).

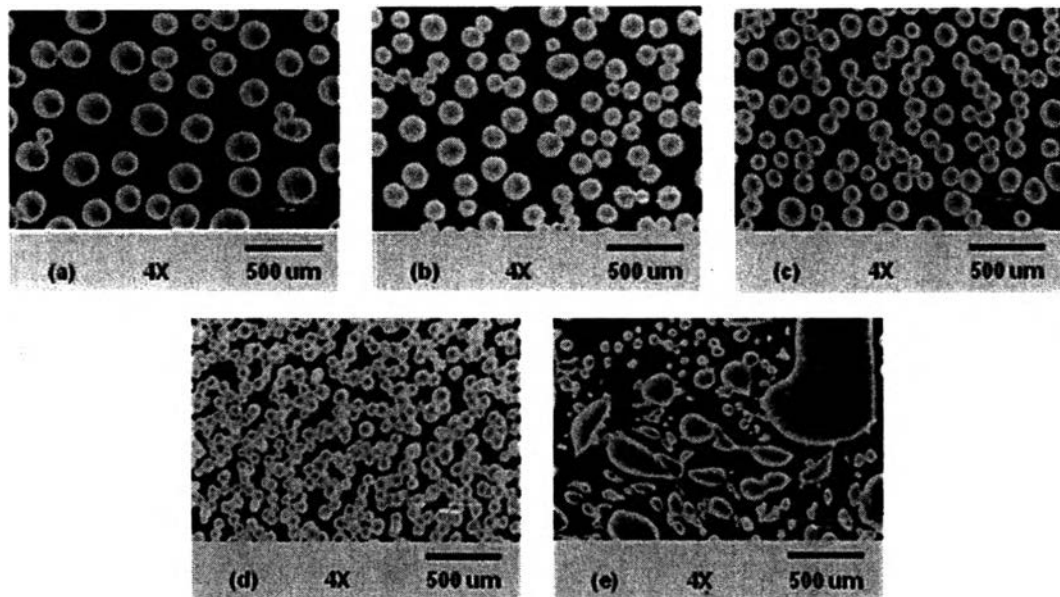


Figure 4.3 OM micrographs of voided HDPE films: (a) 0.5 % ACA, (b) 1 % ACA, (c) 1.5 % ACA, (d) 2 % ACA, and (e) 2.5 % ACA.

Consequently, voided HDPE films with concentration 0.5 %, 1 %, 1.5 % and 2 % were chosen for further study.

Figure 4.4 shows OM micrographs of voided PP films at various concentrations of blowing agent. The micrographs reveal the same trend of the cell size as voided HDPE films. Voided PP films showed irregular structure at 2 % ACA, which was lower than HDPE because it has lower melt strength. Low viscosity and low melt strength lead to a rupture of the cell walls under the elongational forces occurring during cell growth. As a result, the final foam has a high amount of coalesced and open cells (Stange, J., and Munstedt, H., 2006).

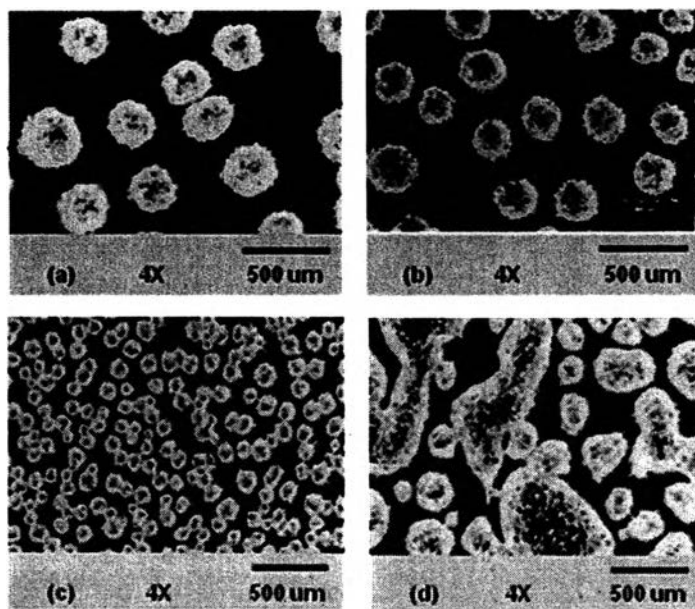


Figure 4.4 OM micrographs of voided PP films: (a) 0.5 % ACA, (b) 1 % ACA, (c) 1.5 % ACA, and (d) 2 % ACA.

Therefore, voided PP films with concentration of 0.5 %, 1 % and 1.5 % were chosen for further study.

B. Density and Porosity

As expected, the densities of voided HDPE films decreased compared to dense film. Increasing blowing agent concentration decreased the density due to more bubbles inside the structure while the porosity increased. Densities and porosities at various ACA concentrations were shown in Table 4.1.

Table 4.1 Average densities and porosities of dense and voided HDPE films at various blowing agent concentrations

Sample	Average density (g/cc)	Porosity (%)
Dense film	0.9491	0
Voided HDPE film, 0.5 % ACA	0.8122	16.5
Voided HDPE film, 1 % ACA	0.8059	17.1
Voided HDPE film, 1.5 % ACA	0.7383	24.1
Voided HDPE film, 2 % ACA	0.7341	24.5

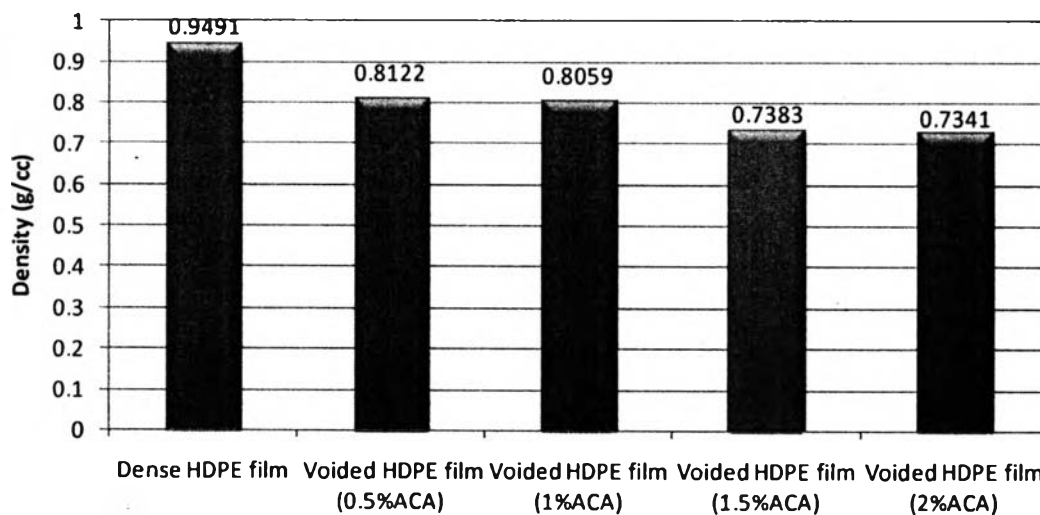


Figure 4.5 Average densities of dense and voided HDPE films at various blowing agent concentrations.

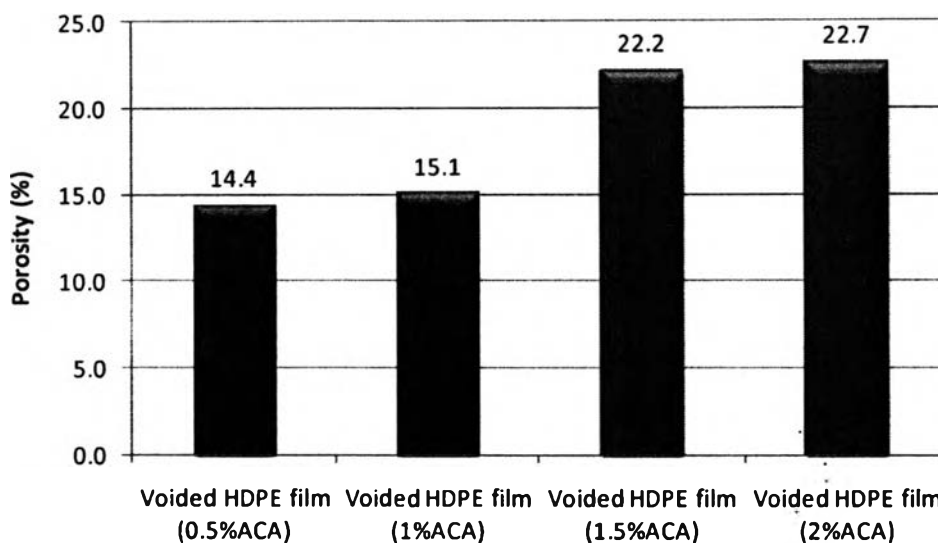


Figure 4.6 Porosities of voided HDPE films at various blowing agent concentrations.

The density of voided PP films also decreased compared to dense film. Increasing blowing agent concentration decreased the density; however, the density increased again when ACA is 1.5%. It is due to incomplete decomposition of ACA content during compression molding. ACA has the density of 1.63 g/cc. When it is mixed with PP, the density of the compound will increase. If all content of ACA can decompose to be gas, the density of the film will decrease compared to dense film.

Table 4.2 Average densities and porosities of dense and voided PP films at various blowing agent concentrations

Sample	Average density (g/cc)	Porosity (%)
Dense film	0.8963	0
Voided PP film, 0.5 % ACA	0.7799	13.0
Voided PP film, 1 % ACA	0.7465	16.7
Voided PP film, 1.5 % ACA	0.7854	12.4

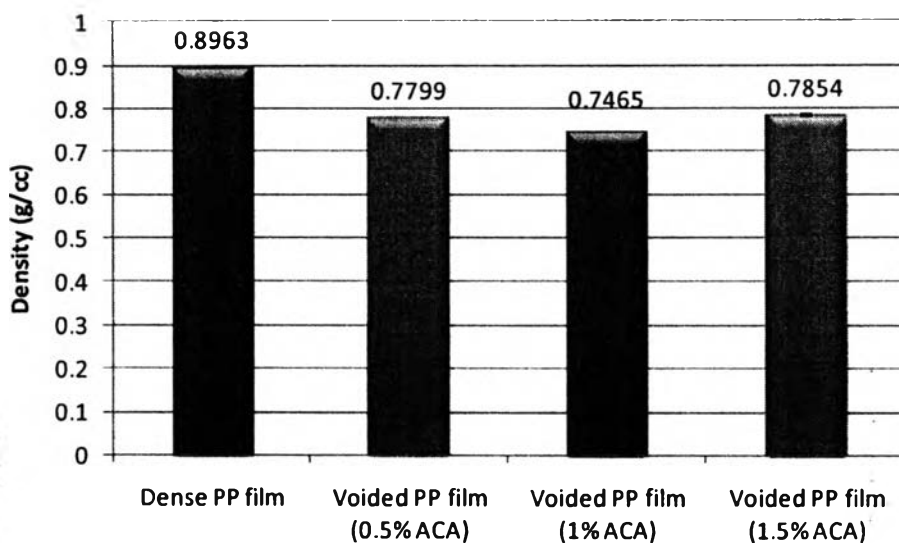


Figure 4.7 Average densities of dense and voided PP films at various blowing agent concentrations.

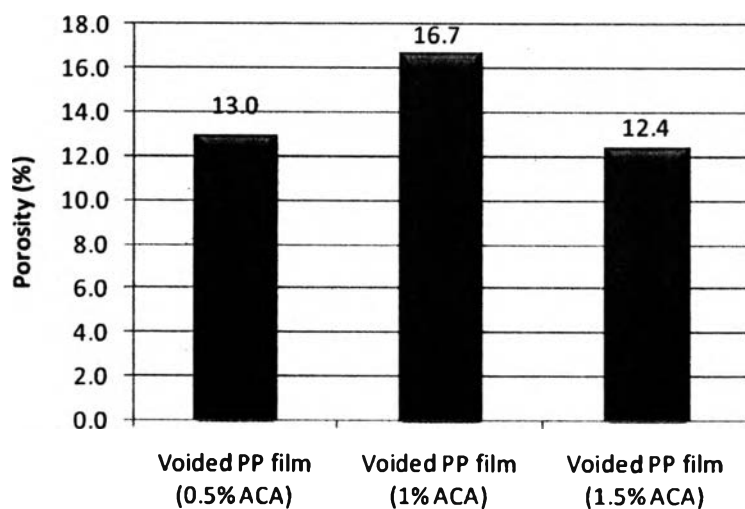


Figure 4.8 Porosities of voided PP films at various blowing agent concentrations.

ATR FT-IR was used to confirm the existence of ACA in compressed PP–1.5 % ACA compounds. The chemical structure of azodicarbonamide is shown in Figure 4.9.

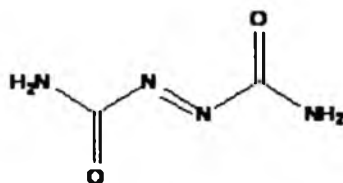


Figure 4.9 Chemical structure of azodicarbonamide.

Figure 4.10 shows the additional peaks at 1690 cm^{-1} and $3100\text{--}3350\text{ cm}^{-1}$ in voided PP film of 1.5 % ACA which were assigned to the C=O stretch in carbonyl compound and --NH_2 in primary amides respectively. However these peaks were not found in spectra of dense, porous film of 0.5 and 1% ACA. The spectrum of voided PP film with 1.5% ACA points out that there is an existence of ACA after the compression.

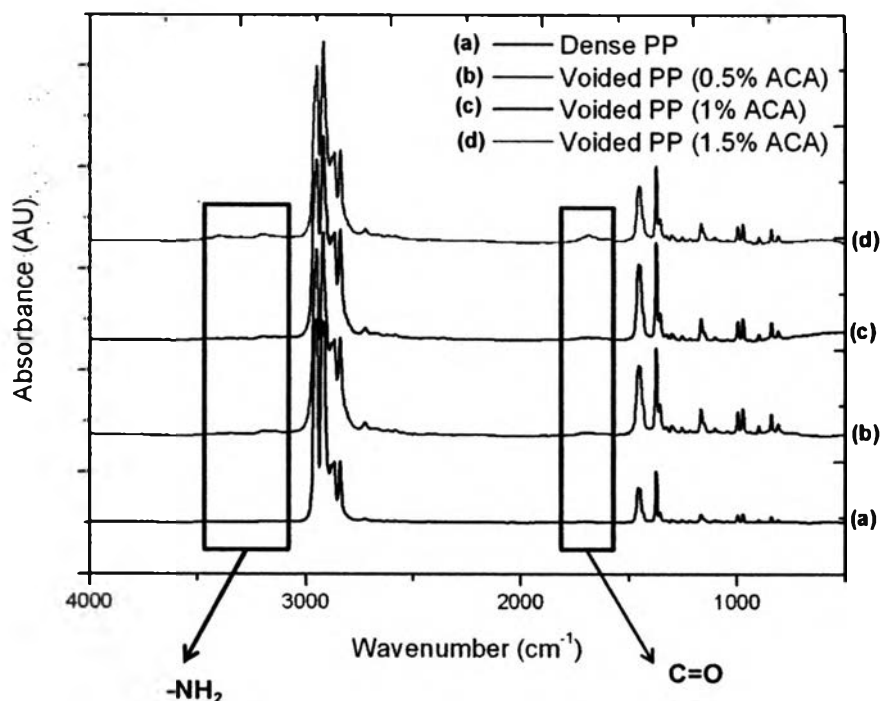


Figure 4.10 FT-IR spectra of PP films: (a) dense, (b) voided of 0.5% ACA, (c) voided of 1 % ACA, and (d) voided of 1.5 % ACA.

As conclusion, voided PP films with concentration 0.5 %, 1 % ACA were suitable for further study.

C. Void Size

The effect of ACA concentration on void size was observed in Tables 4.3 and 4.4. It can be noted that average void size was found to decrease with increased ACA concentration.

Table 4.3 Average void diameters of dense and voided HDPE films at various blowing agent concentrations

Sample	Average void diameter (μm)
Voided HDPE film, 0.5 % ACA	171.75 \pm 37.53
Voided HDPE film, 1 % ACA	126.67 \pm 26.34
Voided HDPE film, 1.5 % ACA	115.14 \pm 23.23
Voided HDPE film, 2 % ACA	56.05 \pm 12.31

Table 4.4 Average void diameters of dense and voided PP films at various blowing agent concentrations

Sample	Average void diameter (μm)
Voided PP film, 0.5 % ACA	320.90 \pm 23.82
Voided PP film, 1 % ACA	265.00 \pm 16.90

4.4.2.2 Thermal Properties

A. Thermogravimetric Analyzer (TGA)

The thermal decomposition of dense and voided films with various blowing agent concentrations was determined by TG-DTA.

Figures 4.11 and 4.12 show TGA thermograms of weight loss versus temperature of HDPE and PP films respectively. The onset decomposition temperatures (T_d) of voided HDPE and PP films were not different from those of dense films in range 458.6 °C to 460.4 °C and 420.0 °C to 422.3 °C respectively. It

can be suggested that the decomposition temperatures of voided films were not depend on the amount of inside air and density of film.

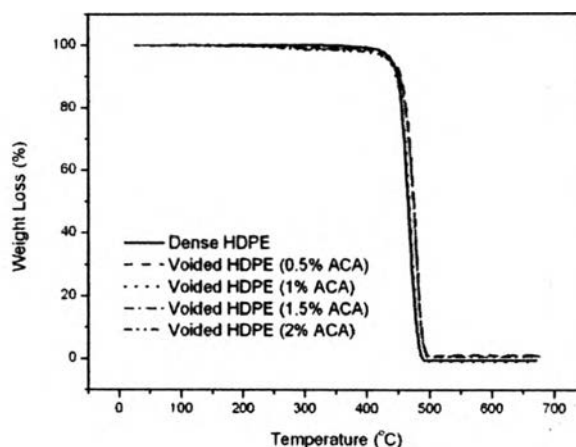


Figure 4.11 TGA thermograms of dense and voided HDPE films at various blowing agent concentrations.

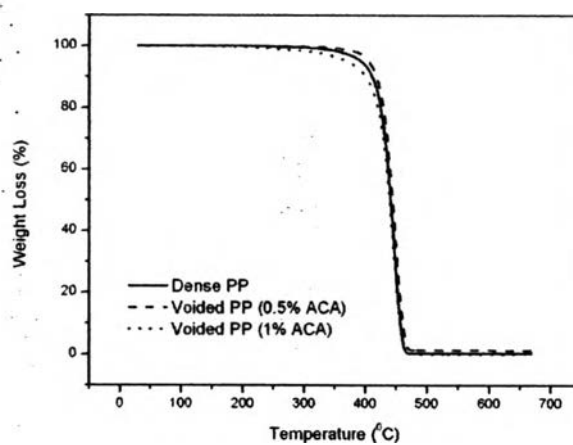


Figure 4.12 TGA thermograms of dense and voided PP films at various blowing agent concentrations.

B. Differential Scanning Calorimeter (DSC)

The DSC graphs of exothermic and endothermic represent crystallization temperature (T_c) and melting temperature (T_m) respectively. They show that crystallization and melting temperatures of voided HDPE films were not different

when compared to those of dense film in range 114.8 °C to 117.1 °C and 131.9 °C to 132.5 °C as shown in Figures 4.13 and 4.14 respectively.

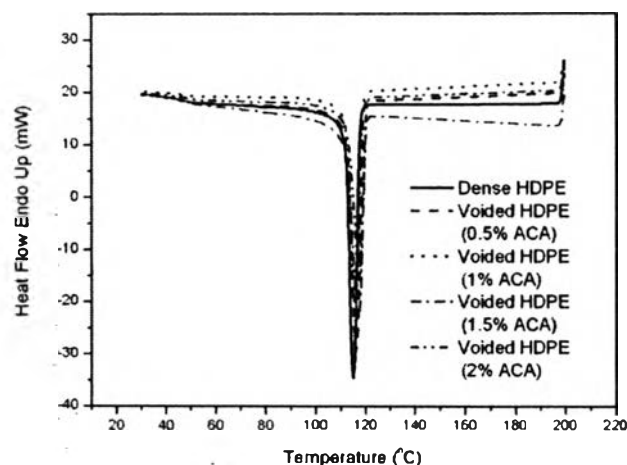


Figure 4.13 DSC graphs of crystallization temperatures of dense and voided HDPE films at various blowing agent concentrations.

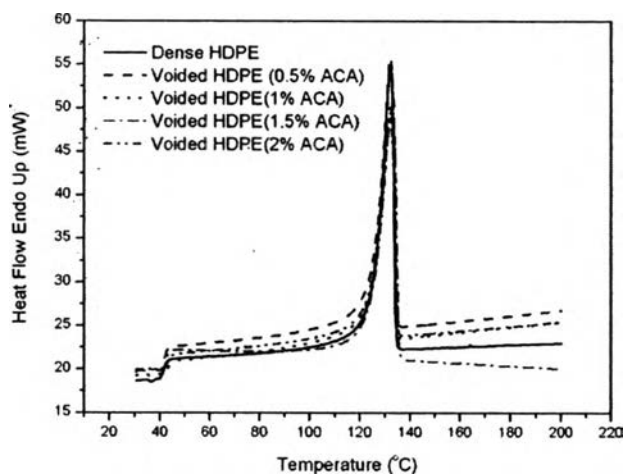


Figure 4.14 DSC graphs of melting temperatures of dense and voided HDPE films at various blowing agent concentrations.

Figures 4.15 and 4.16 show the DSC graphs of PP films. They showed that crystallization and melting temperatures of voided PP films were in range 114.1 °C to 115.8 °C and 156.2 °C to 158.4 °C respectively.

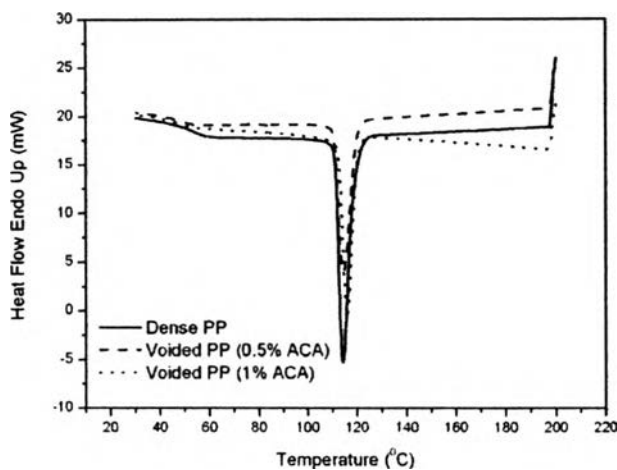


Figure 4.15 DSC graphs of crystallization temperatures of dense and voided PP films at various blowing agent concentrations.

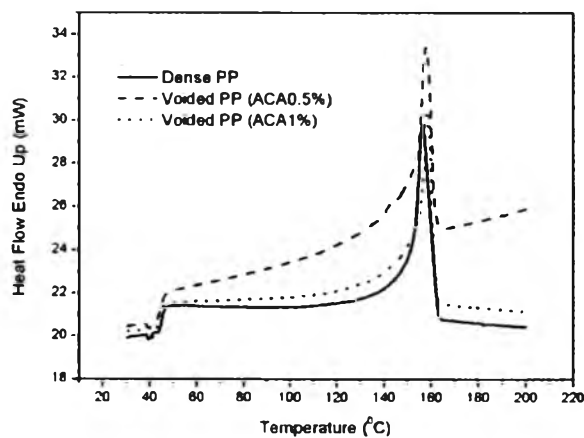


Figure 4.16 DSC graphs of melting temperatures of dense and voided PP films at various blowing agent concentrations.

From all DSC graphs, they were obviously found that thermal properties of voided films were not different from dense films because there was no interaction or chemical bonding between generated voids and polymer matrix.

4.4.2.3 Mechanical Properties

A. Flexural Testing

Flexural strength shows the material's ability to resist deformation under load and flexural modulus is the tendency for the material to resist bending.

Figures 4.17 and 4.18 reveal the decreasing of flexural strength and flexural modulus of voided HDPE when blowing agent concentration increased because of higher porosity content. From the results, it was observed that flexural strength and flexural modulus were inversely proportional to the porosity.

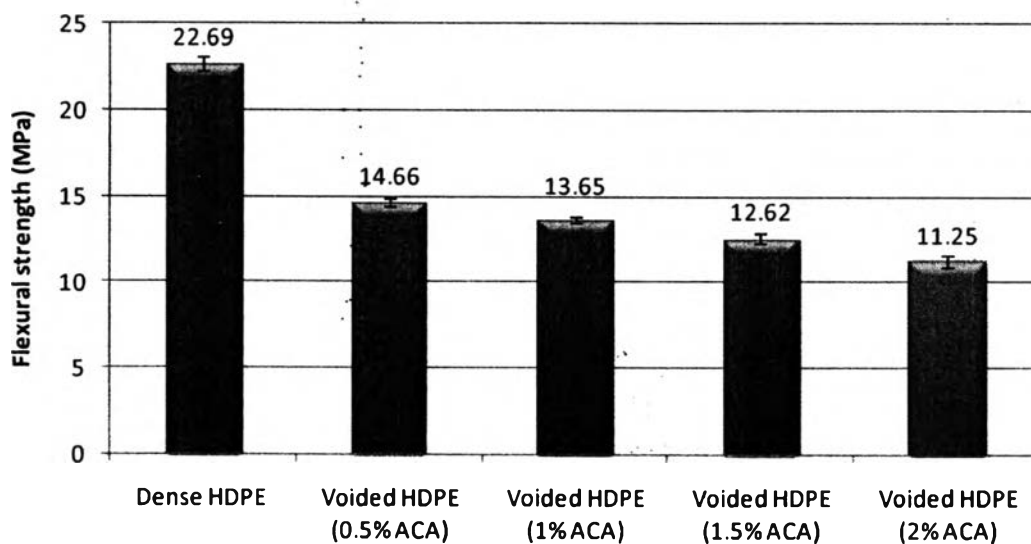


Figure 4.17 Flexural strength of dense and voided HDPE films at various blowing agent concentrations.

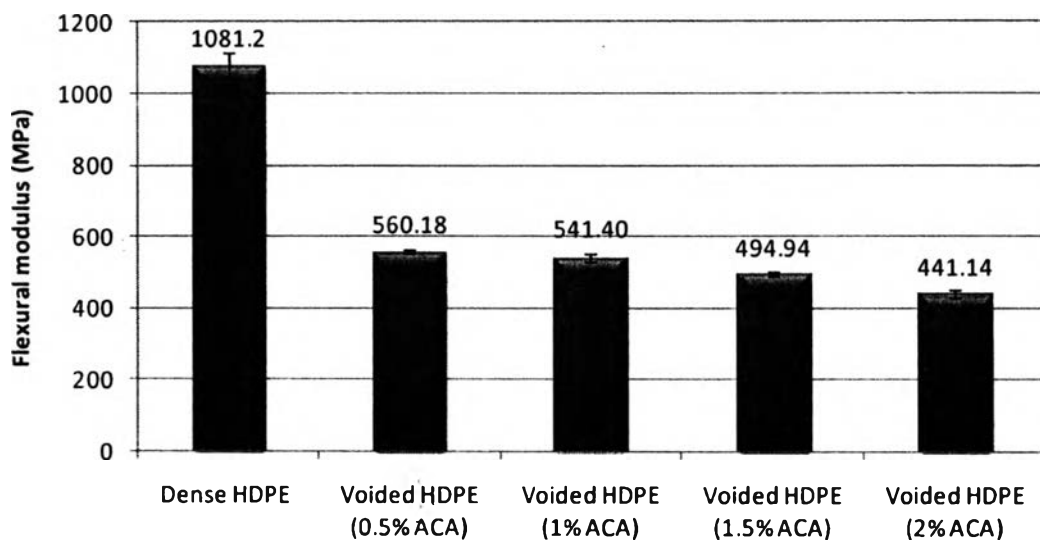


Figure 4.18 Flexural modulus of dense and voided HDPE films at various blowing agent concentrations.

Dense and voided PP samples were also observed the inverse proportionality between porosity and flexural properties as shown in Figures 4.19 and 4.20.

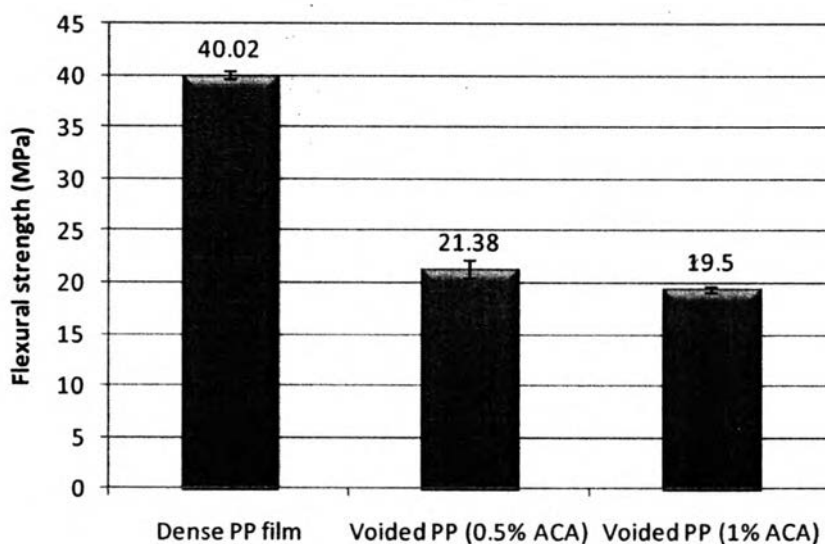


Figure 4.19 Flexural strength of dense and voided PP films at various blowing agent concentrations.

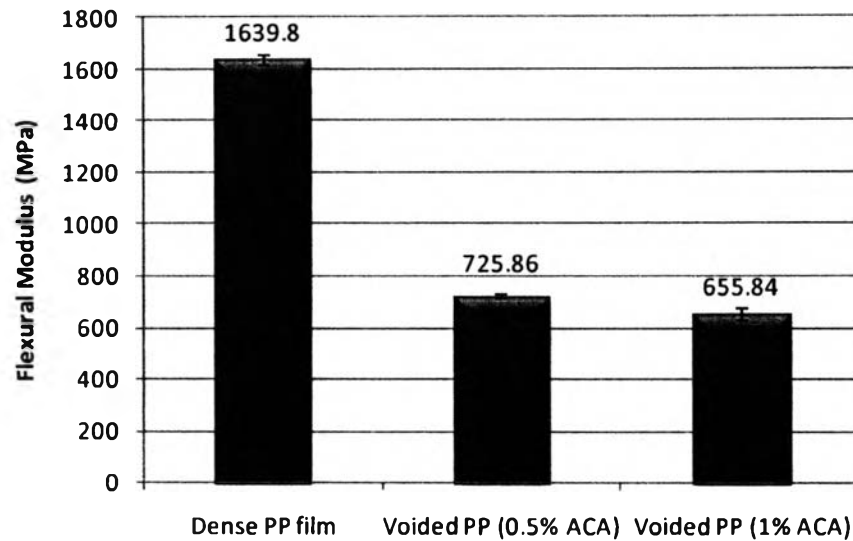


Figure 4.20 Flexural modulus of dense and voided PP films at various blowing agent concentrations.

Although the results of flexural strength in voided HDPE and PP decrease compared to dense samples, they still have enough strength in some applications such as smartcard. The applied force that makes the button of smartcard depleted is 1.28-1.34 N on the area 42 mm² so it is in the range, 0.030 MPa to 0.032 MPa. The calculated values showed that they were too lower than the flexural strength in the prepared voided films.

B. Tensile Testing

Dense HDPE and PP films showed a ductile fracture behavior while voided HDPE and PP films showed a brittle fracture behavior. Elongation at break of voided HDPE films abruptly decreased compared to dense film because the addition of voids in the system will increase the brittleness. This could explain why many ductile materials such as HDPE and PP lose tensile characteristics such as gross necking and elongation characteristic after foaming and behave as brittle materials (Zhang, Y. *et al.*, 2003).

The voided HDPE films show lower stiffness and higher brittleness than dense film as shown in Figures 4.22 and 4.23 by the decrease in the stress at break and in the strain at break values, respectively. From Figure 4.21, it was found that the

creation of voids decrease the tensile modulus of the films. The higher the porosity, the lower the tensile properties were obtained. However, the results of relative tensile strain at break of voided films with various ACA concentrations were not significantly different.

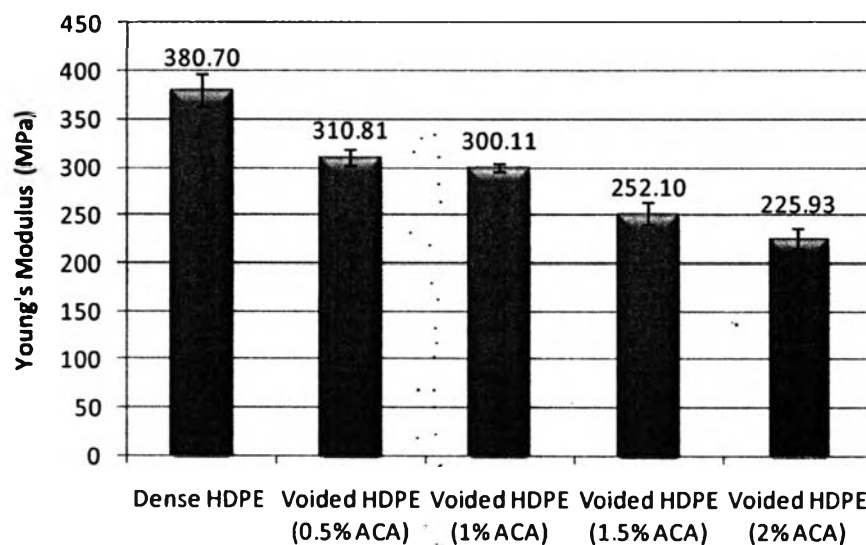


Figure 4.21 Young's modulus of dense and voided HDPE films at various blowing agent concentrations.

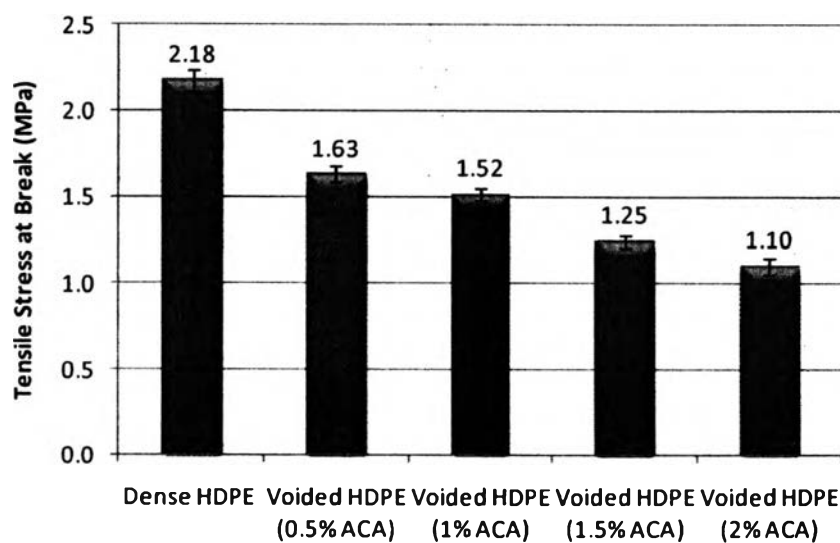


Figure 4.22 Tensile stress at break of dense and voided HDPE films at various blowing agent concentrations.

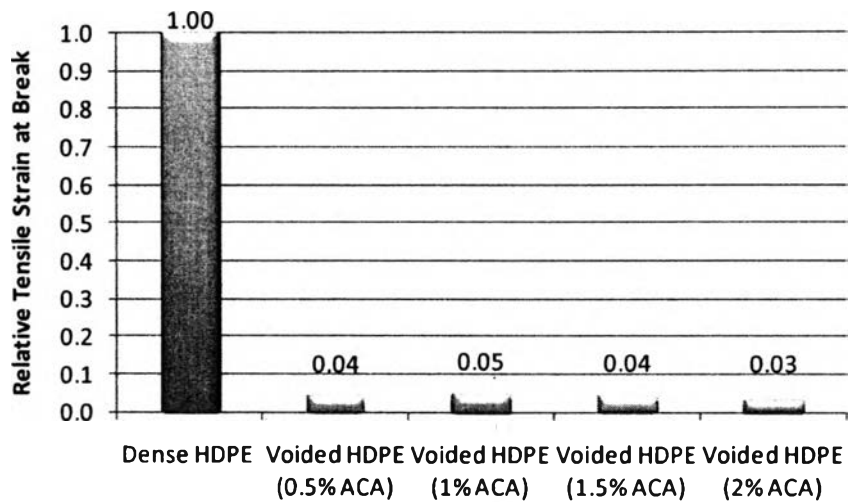


Figure 4.23 Relative tensile strain at break of dense and voided HDPE films at various blowing agent concentrations.

Figures 4.25 and 4.26 show the decreasing in the stress at break and strain at break value in voided PP films compared to dense film. The results were lowest in voided PP Film with 0.5 % ACA compared to 1 % ACA implied that the void size has more effect on both properties in voided PP film than the porosity. From Figure 4.24, it was found that the creation of voids decrease the Young’s modulus of the films. Increasing blowing agent concentrations showed the lower Young’s modulus.

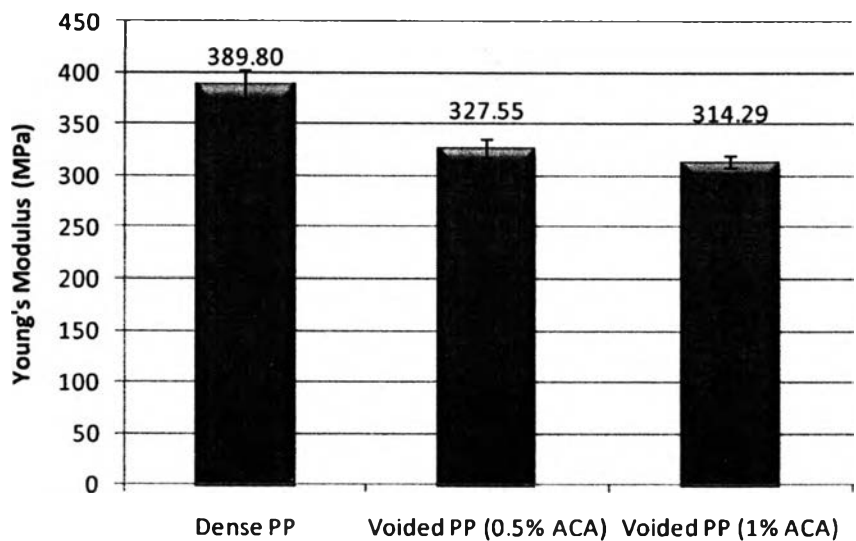


Figure 4.24 Young’s modulus of dense and voided PP films at various blowing agent concentrations.

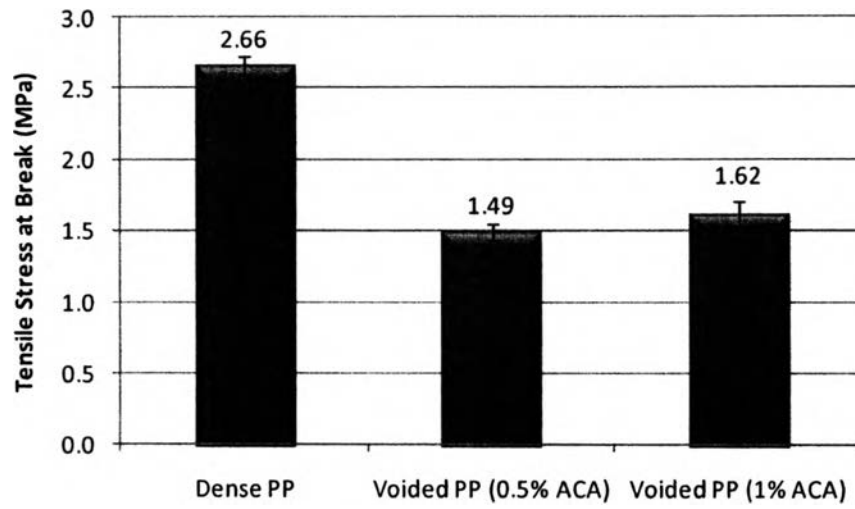


Figure 4.25 Tensile stress at break of dense and voided PP films at various blowing agent concentrations.

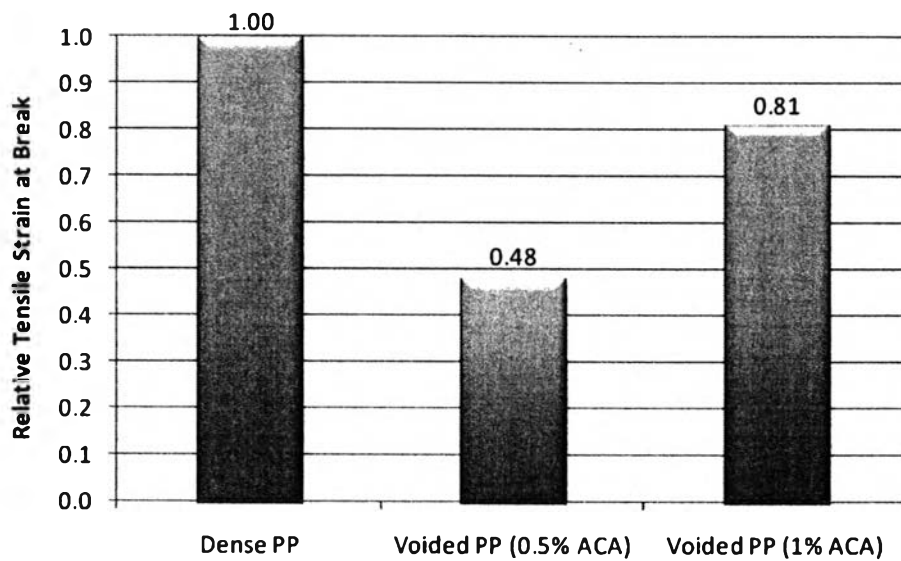


Figure 4.26 Relative tensile strain at break of dense and voided PP films at various blowing agent concentrations.

4.4.2.4 Electrical Properties

A. Dielectric strength

The existence of a maximum voltage which a material will support for a long time without failing is dielectric strength defined as the breakdown voltage divided by the thickness (Blythe, T., and Bloor, D, 2005).

Voided HDPE and PP films had lower dielectric strengths compared to dense films because of the presence of voids. Peacock, A. (2000) reported that the dielectric strength is influenced by the presence of contaminants such as dirt or void. In most cases, inhomogeneities within the chemical and physical structure reduce dielectric strength.

Table 4.5 shows dielectric strength of dense and voided HDPE films and Table 4.6 of dense and porous PP films. The results were observed the lower dielectric strength when increasing blowing agent concentrations. This was due to higher amount of gas inside the films.

Table 4.5 Average dielectric strengths of dense and voided HDPE films at various blowing agent concentrations

Sample	Average dielectric strength (MV/m)
Dense film	10.04 ± 0.46
Voided HDPE film, 0.5% ACA	9.45 ± 0.31
Voided HDPE film, 1% ACA	8.25 ± 0.38
Voided HDPE film, 1.5% ACA	6.75 ± 0.28
Voided HDPE film, 2% ACA	5.78 ± 0.35

Table 4.6 Average dielectric strengths of dense and voided PP films at various blowing agent concentrations

Sample	Average dielectric strength (MV/m)
Dense film	11.15 ± 0.11
Voided PP film, 0.5% ACA	6.96 ± 0.31
Voided PP film, 1% ACA	5.36 ± 0.22

Dielectric strength of voided HDPE films gradually decreased while the values of voided PP significantly reduced. It causes from very weak melt strength of PP. When the melt strength is too weak, the cell walls may not have enough strength to bear the extensional force and may rupture very easily (Xu, Z-M. *et al.*, 2007).

The breakdown occurred at the border of all dense films but inside of all voided films.

There are 4 principal mechanisms of electrical breakdown in solid polymers which are electronic breakdown, electromechanical breakdown, thermal breakdown and breakdown caused by gas discharged. Organic polymers are especially prone to the last mechanism, because bombardment of the polymer molecules by ions in the discharge is able to break chemicals bonds. The reactive free radicals thereby produced, together with any available oxygen (often dissolved in the polymer), enter into the degradative chain reaction, causing damage to the sample. It can be divided into two types. First, internal discharges and electrical treeing are the mechanism of breakdown in the voided films. Voids are created inside the materials and the relative permittivity of gas filling a void is generally less than that of polymer. So the electric field in void will be greater than the field in the surrounding medium. Second, external discharges and surface tracking caused the breakdown in the dense films (Blythe, T., and Bloor, D, 2005)

B. Dielectric constant and dielectric loss

Figure 4.27 shows dielectric constant and dielectric loss from 1 kHz to 1 MHz of dense and voided HDPE films and Figure 4.28 of dense and voided PP films. They were found that the dielectric constants of dense and voided films exhibited low frequency dependence. The variation in dielectric constant with frequency indicated the presence of an interfacial polarization in the polymer matrix. This slightly decreased dielectric constant with increased frequency is thought to be caused by the slow dielectric relaxation of the matrix resin (Sui, G. *et al.*, 2008). The introduction of voids into the films considerably reduced dielectric constant because the voids behaved like an air which has dielectric constant of 1. The higher blowing agent concentration seemed to give lower dielectric constant due to higher fraction of

air in the films. Very low dielectric losses of voided films show that there was no voids on the surface of the voided films but the voids were created only inside the film.

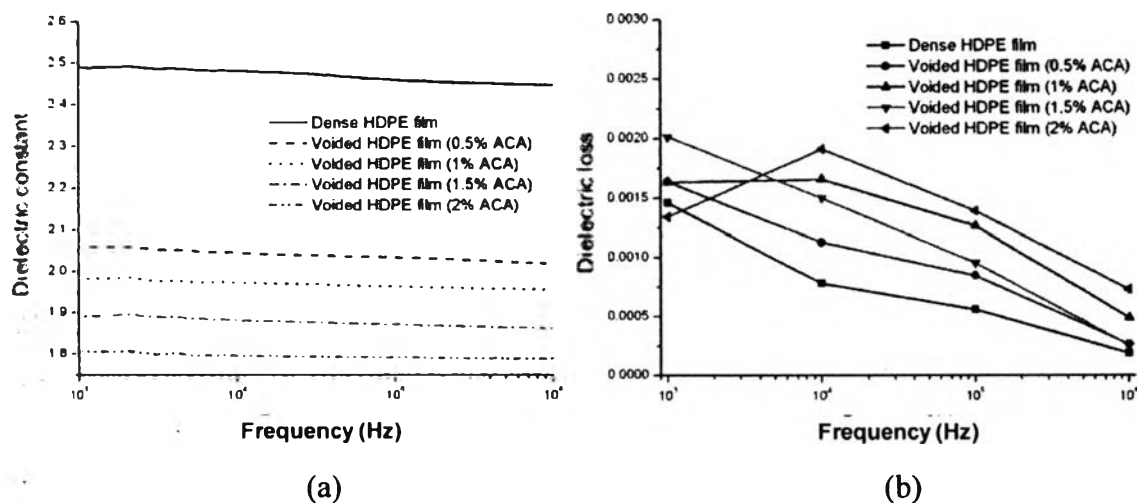


Figure 4.27 (a) Dielectric constant and (b) dielectric loss as a function of frequency at room temperature of dense and voided HDPE films.

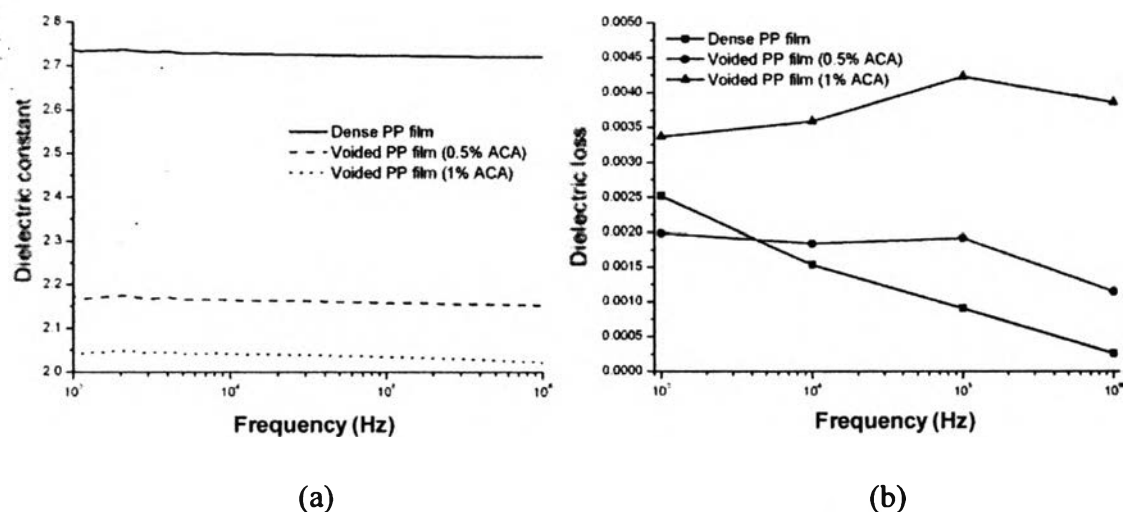


Figure 4.28 (a) Dielectric constant and (b) dielectric loss as a function of frequency at room temperature of dense and voided PP films.

Dielectric constants and dielectric losses were also measured as a function of temperatures from -70 °C to 110 °C for HDPE and from -40 °C to 130 °C for PP. From the material specifications, glass transition temperatures (T_g) of HDPE and PP

were $-10\text{ }^{\circ}\text{C}$ and $-60\text{ }^{\circ}\text{C}$, respectively. Below T_g , the molecular chains of polymers were frozen while the mobility of polymers chains increases above this temperature. From 4.29 and 4.30, the slight increasing of dielectric constant above T_g was observed. At temperatures higher than T_g , the dielectric constant almost unaffected with temperature. Daniels C.A. (1989) reported that polymers that do not have a dipolar structure and are free of other sources of dipoles display a consistently value for the dielectric constant, which does not change with frequency and temperature. The independence of dielectric constant and dielectric loss on temperature, suggesting that voided HDPE and PP films can be used in broad ranges of frequency and temperature.

When polymers possess very no polar groups such as HDPE and PP, dielectric relaxation may be very weak effects, which are scarcely observed, although the underlying molecular rearrangement processes will still be there. In these circumstances it is often possible to enhance the dielectric effect by adding just a few polar groups, which in other way do not disturb the system too much (Blythe, T., and Bloor, D, 2005).

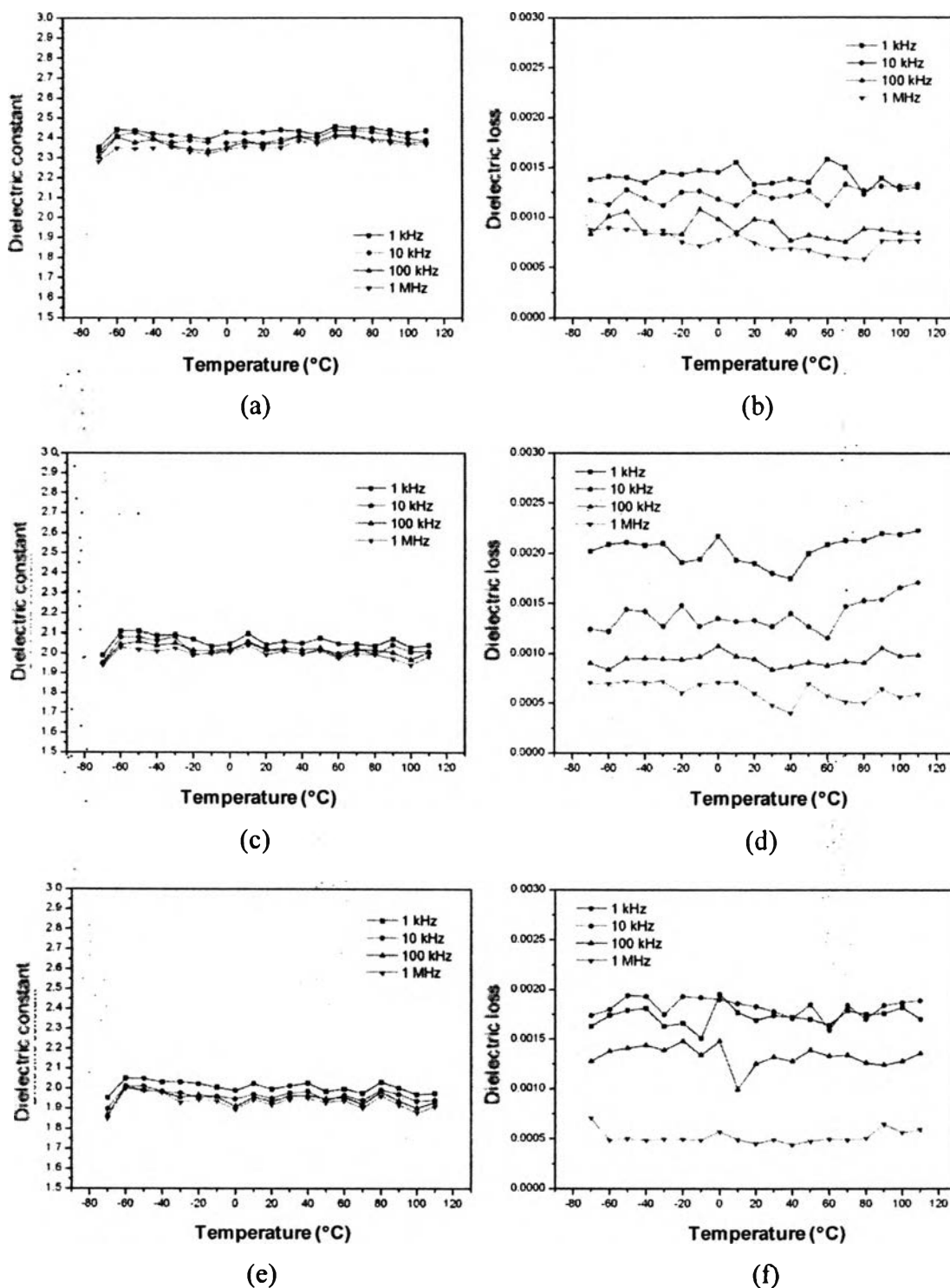


Figure 4.29 Dielectric constant and dielectric loss as a function of temperatures at different frequencies of (a) and (b) dense HDPE film, (c) and (d) voided HDPE film of 0.5 % ACA, and (e) and (f) voided HDPE of 1 % ACA.

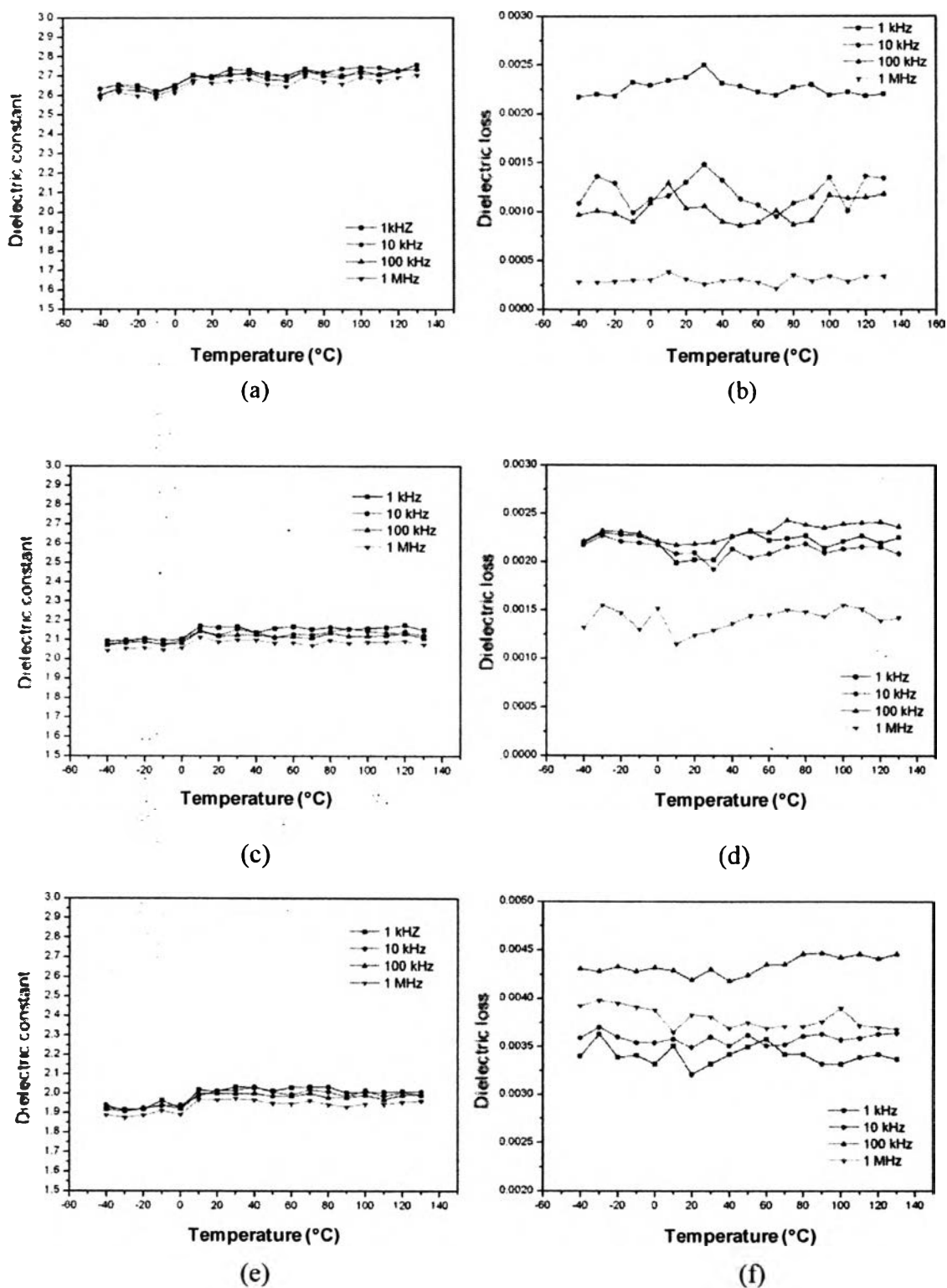


Figure 4.30 Dielectric constant and dielectric loss as a function of temperatures at different frequencies of (a) and (b) dense PP film, (c) and (d) voided PP film of 0.5 % ACA, and (e) and (f) voided PP film of 1 % ACA.

Figures 4.31 and 4.32 show OM micrographs of voided HDPE of 0.5 % ACA and voided PP of 1 % ACA at different temperatures. From all micrographs, it can be concluded that there was no change in the structure of voids from 30 °C to 110 °C in HDPE and from 30 °C to 130 °C in PP. It was due to these temperature ranges were below the melting temperature of both polymers.

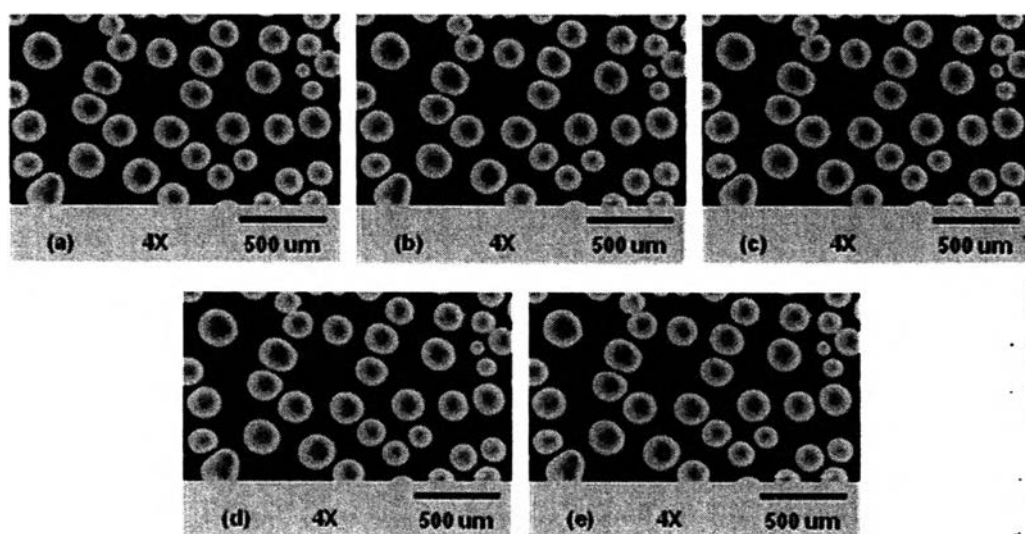


Figure 4.31 OM micrographs of voided HDPE films of 0.5 % ACA at different temperatures: (a) 30 °C, (b) 50 °C, (c) 70 °C, (d) 90 °C, and (e) 110 °C.

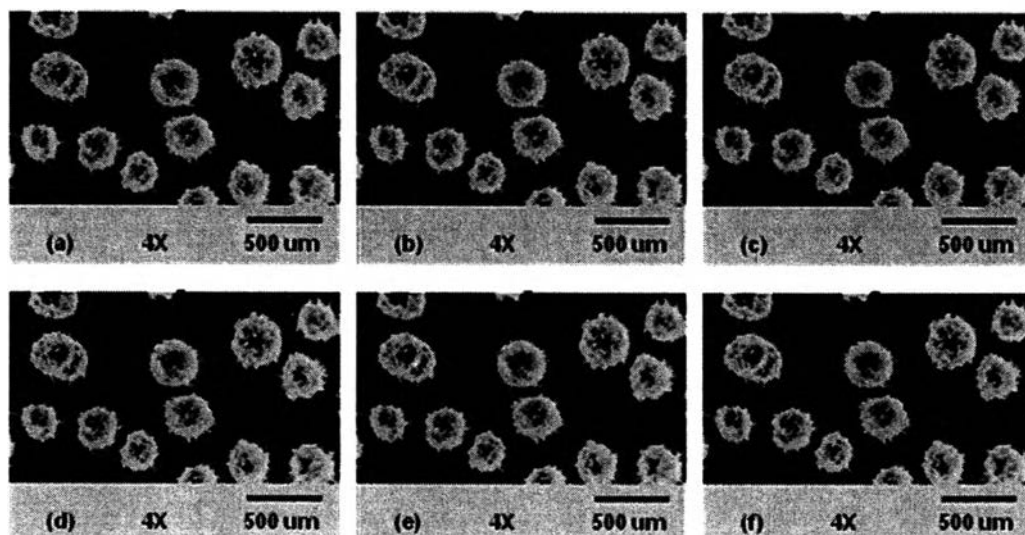


Figure 4.32 OM micrographs of voided PP films of 1 % ACA at different temperatures: (a) 30 °C, (b) 50 °C, (c) 70 °C, (d) 90 °C, (e) 110 °C, and (f) 130 °C.

Zhang, H. *et al.* (2008) reported that the overall dielectric constant depends on two aspects. One is the dielectric constants of the dense material and the voids. The other is the proportion and geometrical structures of them. Generally, void size showed little effect on the overall dielectric constant for it cannot directly affect the two aspects. But from this point of view, porosity and void shape directly affect the proportion of the voids and the geometrical structures, respectively. Therefore, in consideration of the same spherical void shape of each sample, porosity was taken as the key influential factor on the dielectric constant

The two extreme models are the parallel and the serial models. Parallel model can well describe the dielectric constant of porous films that contain voids extending mostly from the bottom to the top surface. If the films have uniformly distributed voids with closed air gaps, the dielectric constant is better expressed by the Serial model. The other two models are Rayleigh model and Lorentz–Lorentz model. Rayleigh model assumes a cubic array of spherical voids while Lorentz–Lorentz model has no restriction to void shapes. Their equations are expressed by

$$\varepsilon^v = \varepsilon^v_{\text{void}} + \varepsilon^v_{\text{dense}}(1-P) \quad v = 1 \text{ for parallel model} \quad (1)$$

$$v = -1 \text{ for serial model} \quad (2)$$

$$\varepsilon_{\text{Rayleigh}} = \varepsilon_{\text{dense}} - \frac{3\varepsilon_{\text{dense}} P(\varepsilon_{\text{dense}} - \varepsilon_{\text{pore}})}{2\varepsilon_{\text{dense}} + \varepsilon_{\text{pore}} + P(\varepsilon_{\text{dense}} - \varepsilon_{\text{pore}})} \quad (3)$$

$$\varepsilon_{\text{Lorentz-lorentz}} = \frac{(\varepsilon_{\text{dense}}(\varepsilon_{\text{pore}} + 2) - 2P(\varepsilon_{\text{dense}} - \varepsilon_{\text{pore}}))}{\varepsilon_{\text{pore}} + 2 + P(\varepsilon_{\text{dense}} - \varepsilon_{\text{pore}})} \quad (4)$$

where ε is the overall dielectric constant. $\varepsilon_{\text{dense}}$ and $\varepsilon_{\text{void}}$ are the dielectric constants of the dense material and the void (air), respectively. P is the porosity (Zhang, H., *et al.*, 2008).

As shown in Figures 4.33 and 4.34, the experimental data close to the Serial model. It was in agreement with the OM micrographs and the Serial's assumptions. Therefore, we ascribe this correlation mainly to the uniform distribution of voids with closed air-gaps.

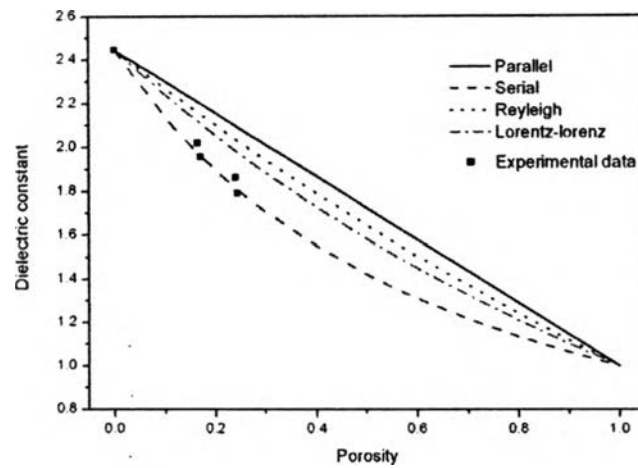


Figure 4.33 Correlation between the dielectric constant at 1 MHz and porosity of voided HDPE films at room temperature as calculated as according to different model.

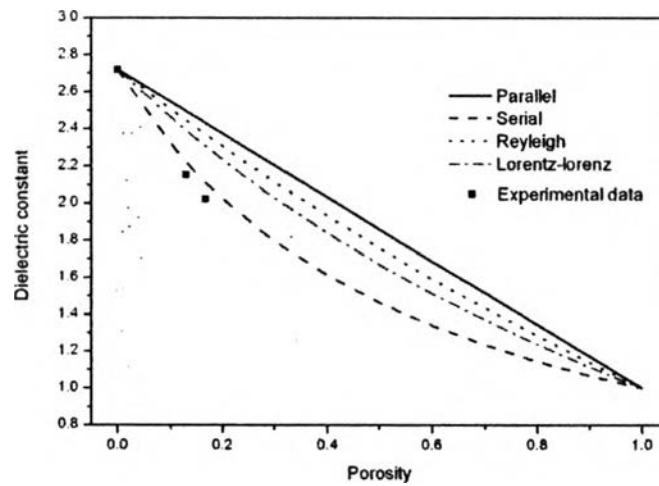


Figure 4.34 Correlation between the dielectric constant at 1 MHz and porosity of voided PP films at room temperature as calculated as according to different model.

C. Piezoelectric coefficient

The internal voids could enhance piezoelectric coefficient in non-polar polymers because electrical charging yields charge separation inside the void and charge storage on the electrets material surrounding the voids. Often a corona discharge is used for charging (Gerhard-Mulhaupt, R., *et al.*, 2002).

Poling of all samples was performed by corona discharge of 20 kV/mm. Corona poling was carried out in atmosphere air at a relative humidity of 44 % to 52 %. The applied voltage higher than 20 kV/mm caused the breakdown in voided samples, respectively. Tables 4.8 and 4.9 show that the poling did not cause the piezoelectric properties in dense HDPE and PP films while the same poling condition in the voided films showed piezoelectric properties. Voided HDPE film of 2 % ACA showed the highest value which was 4 pC/N. There are two possible reasons that make the highest piezoelectric constant in the voided HDPE film of 2 % ACA. First, it had the highest surface area of voids per the same sample area which make the highest area for charge trapping. Second, piezoelectric coefficient is inversely proportional to Young's modulus (Lushcheikin, G.A., 2006). The lowest Young's modulus was measured in this film so it showed the highest value of piezoelectric coefficient.

Table 4.7 Surface area of voids per sample area 1 cm²

Sample	Surface area of voids (cm ²)
Voided HDPE film, 0.5 % ACA	1.44
Voided HDPE film, 1 % ACA	1.52
Voided HDPE film, 1.5 % ACA	1.58
Voided HDPE film, 2 % ACA	1.67
Voided PP film, 0.5 % ACA	1.33
Voided PP film, 1 % ACA	1.42

Table 4.8 Piezoelectric coefficients of dense and voided HDPE films at various blowing agent concentrations

Sample	Piezoelectric Coefficient (pC/N)	
	Before Poling	After Poling
Dense film	0	0
Voided HDPE film, 0.5 % ACA	0	2
Voided HDPE film, 1 % ACA	0	3
Voided HDPE film, 1.5 % ACA	0	3
Voided HDPE film, 2 % ACA	0	4

Table 4.9 Piezoelectric coefficients of dense and voided PP films at various blowing agent concentrations

Sample	Piezoelectric Coefficient (pC/N)	
	Before Poling	After Poling
Dense film	0	0
Voided PP film, 0.5 % ACA	0	1
Voided PP film, 1 % ACA	0	2

4.5 Conclusions

The spherical voided HDPE and PP films were produced by blowing agent (azodicarbonamide or ACA) compression molding. The higher ACA concentration can yield a lower void size and density but higher porosity. The creation of internal voids did not effect to the thermal properties of the polymers. The mechanical properties of voided films lower than those of dense films. Voided films with higher density showed better mechanical properties. The dielectric constants of voided films lower than those of dense films because the voids behaved like an air which has dielectric constant of 1. The voided films can be described as 0–3 void–polymer composites from fitting the data of dielectric mixing. The measured dielectric constants could fit with Serial model indicating the uniform distribution of voids with closed air-gaps. Low dielectric losses of voided films show that there was no voids on the surface of the voided films but the voids were created only inside the film. Poling of voided films show the values of piezoelectric coefficient because

electrical charging yields charge separation inside the voids and charges can store surrounding the voids lead to the induced dipole inside the structure of voided films.

4.6 Acknowledgements

I would like to thank Dr. Pitak Laoratanakul, Dr. Aree Thanaboonsombut and MTEC staffs for their kindness for the instrument support and the useful training. Also thank Asst. Prof. Rattikorn Yimnirun for his suggestion and endless kindness for the instrument support.

In addition, I would like to take this opportunity to thank Thai Polyethylene Co., Ltd. for providing the HDPE and PP resin and Usaco (Thailand) Co., Ltd. for providing the azodicarbonamide.

Finally, the author is grateful for the scholarship and funding of the thesis work provided by the Petroleum and Petrochemical College, and by the National Center of Excellence for Petroleum, Petrochemicals, and Advanced Materials, Thailand.

4.7 References

1. Bauer, S., Bauer-Gogonea, S., Dansachmüller, M., Hoislbauer, H., Lindner, M., and Schwödiauer. (2002). Physics of electromechanically active, cellular materials. 11th International Symposium on Electrets, 2002, 50-53.
2. Blythe, T., and Bloor, D. (2005). Electrical Properties of Polymers (Cambridge Solid State Science Series). Cambridge University Press: Cambridge.
3. Daniels, C.A. (1989). Polymers: Structure and Properties. Lancaster: Technomic Publishing.
4. Gerhard-Malthaupt, R., Wegener, M., Wirges, W., Giacometti, J.A. Altafim, R.A.C. (2002). Electrode poling of cellular polypropylene

- films with short-high voltage pulse. 11th International Symposium on Electrets, 2002, 36-45.
5. Lushcheikin, G.A. (2006). New polymer-containing piezoelectric materials. Physics of the Solid State, 48(6), 1023–1025.
 6. Nalwa, H.S. (1995). Ferroelectric Polymers Chemistry, Physics, and Applications. New York: Marcel Dekker.
 7. Peacock, A.J. (2000). Handbook of Polyethylene Structures, Properties, and Applications. New York: Marcel Dekker.
 8. Quinn, S. (2001). Chemical blowing agents: providing production, economic and physical improvements to a wide range of polymers. Plastics Additives & Compounding, 3(5), 16-21.
 9. Stange, J., and Munstedt, H. (2006). Effect of long-chain branching on the foaming of polypropylene with azodicarbonamide. Journal of Cellular Plastics, 42(6), 445-467.
 10. Sui, G., Jana, S., Zhong, W.H., Fuqua, M.A., and Ulven, C.A. (2008). Dielectric properties and conductivity of carbon nanofiber/semi-crystalline polymer composites. Acta Materialia, 56, 2381-2388.
 11. Xu, Z.-M., Jiang, X.-L., Liu, T., Hub, G.-H., Zhao, L., Zhua, Z.-N., and Yuan, W.-K. (2007). Foaming of polypropylene with supercritical carbon dioxide. Journal of Supercritical Fluids, 41, 229-310.
 12. Zhang, H., Zhou, J., Zhang, X., Wang, H., Zhong, W., Du, Q. (2008). High density polyethylene-grafted-maleic anhydride low-k porous films prepared via thermally induced phase separation. European Polymer Journal .44, 1095-1101.

13. Zhang, Y, Rodrigue, D., and Ait-Kadi, A. (2003). High density polyethylene foams. I. Polymer and foam characterization. Journal of Applied Polymer Science, 90(8), 2111-2119.
14. Zhang, Y, Rodrigue, D., and Ait-Kadi, A. (2003). High density polyethylene foams. III. Tensile properties. Journal of Applied Polymer Science, 90(8), 2130-2138.
15. Zhang, Y, Rodrigue, D., and Ait-Kadi, A. (2003). High density polyethylene foams. IV. Flexural and tensile moduli of structural foams. Journal of Applied Polymer Science, 90(8), 2139-2149.